

Do surface temperature indices reflect trends in Atlantic Meridional Overturning Circulation strength?

Christopher M Little¹, Mengnan Zhao², and Martha Weaver Buckley³

¹Atmospheric and Environmental Research, Inc.

²Atmospheric and Environmental Research

³George Mason University

November 23, 2022

Abstract

The difference between North Atlantic subpolar gyre sea surface temperatures (SPG SSTs) and hemispheric- or global-scale surface temperatures has been utilized as an index of centennial-timescale changes in Atlantic Meridional Overturning Circulation (AMOC) strength. Here, using Community Earth System Model ensembles, we show that surface temperature-based indices (STIs) proposed to date largely reflect global-scale temperature trends and thus do not reflect dynamical relationships with AMOC. More broadly, we find that relationships between STIs, SPG SSTs, and AMOC strength differ greatly in significance and magnitude over different time periods because they are dependent upon the nature of external forcing. In the 20th century, characterized by offsetting greenhouse gas and aerosol forcing, the relationship between SSTs and AMOC strength varies widely and changes sign across a 20-member ensemble. We conclude that STIs and SPG SSTs are poor predictors of centennial-timescale AMOC strength variations.

1 **Do surface temperature indices reflect trends in**
2 **Atlantic Meridional Overturning Circulation strength?**

3 **Christopher M. Little¹, Mengnan Zhao¹, Martha W. Buckley²**

4 ¹Atmospheric and Environmental Research, Inc., Lexington, MA, USA.

5 ²George Mason University, Fairfax, VA, USA

6 **Key Points:**

- 7 • Previously proposed surface temperature indices (STIs) of AMOC strength are
8 dominated by global temperature trends
- 9 • STIs are poor predictors of AMOC strength outside their calibration period, call-
10 ing into question previous interpretations of 20th c. trends
- 11 • Over centennial timescales, AMOC/STI relationships are sensitive to the nature
12 of external forcing and unforced variability

Abstract

The difference between North Atlantic subpolar gyre sea surface temperatures (SPG SSTs) and hemispheric- or global-scale surface temperatures has been utilized as an index of centennial-timescale changes in Atlantic Meridional Overturning Circulation (AMOC) strength. Here, using Community Earth System Model ensembles, we show that surface temperature-based indices (STIs) proposed to date largely reflect global-scale temperature trends and thus do not reflect dynamical relationships with AMOC. More broadly, we find that relationships between STIs, SPG SSTs, and AMOC strength differ greatly in significance and magnitude over different time periods because they are dependent upon the nature of external forcing. In the 20th century, characterized by offsetting greenhouse gas and aerosol forcing, the relationship between SSTs and AMOC strength varies widely and changes sign across a 20-member ensemble. We conclude that STIs and SPG SSTs are poor predictors of centennial-timescale AMOC strength variations.

Plain Language Summary

The short observational record of the Atlantic Meridional Overturning Circulation (AMOC) limits our ability to assess changes in its strength over the instrumental and pre-instrumental periods. Indirect proxies of ocean circulation are thus required to make inferences about past trends, e.g. those over the past century. Several previous analyses have used surface temperature indices to interpret 20th century AMOC trends. However, the robustness of this indirect AMOC proxy, including its sensitivity to time period, timescale, and/or climate state, has not been assessed.

We use two state-of-the-art climate model ensembles to assess AMOC/surface temperature relationships over century timescales, finding a strong dependence upon time period and climate forcing. Our results clarify the origins of discrepancies in AMOC/surface temperature relationships and suggest that interpretations of 20th century climate and ocean circulation change based on surface temperature indices are limited.

1 Introduction

Sea surface temperatures (SSTs) are influenced by many factors, including sensible and latent air-sea heat fluxes, short and long wave radiation, and ocean heat transport due to processes such as Ekman pumping, vertical mixing and horizontal advection

(e.g. Bjerknes, 1964; Frankignoul, 1985; Chen et al., 1994; Webster et al., 2005; Pardo & Prez, 2011; Buckley et al., 2014, 2015; Buckley & Marshall, 2016). These factors interact and control SST variability at different scales. Over multidecadal and longer timescales, ocean advection is an important influence on SSTs (Bjerknes, 1964; Gulev et al., 2013). For example, low-frequency, basin-wide, SST changes, commonly referred to as Atlantic Multidecadal Variability, are generally thought to be related to variability of the Atlantic Meridional Overturning Circulation (AMOC) (Delworth et al., 2007; Deser et al., 2010; Zhang et al., 2019) (although recent work has called this assumption into question (Clement et al., 2015)). This implies that SSTs may act as fingerprints of multi-decadal to millennial changes in ocean circulation and climate, for which observational records are limited (Kravtsov & Spannagle, 2008; De Boer et al., 2010; Williams et al., 2014; Rahmstorf et al., 2015; Caesar et al., 2018).

Over centennial timescales, many studies have noted a “warming hole”, or “cold patch”, in the North Atlantic subpolar gyre (SPG). In some model simulations, this SST pattern has been related to changes in the AMOC (Marshall et al., 2015; Winton et al., 2013; Caesar et al., 2018), although other studies indicate that AMOC-SST relationships, including the appearance of the warming hole, depend upon climate forcing (Roberts et al., 2013). In particular, the role of AMOC changes in the warming hole over the 20th century is debated: some studies assert that the warming hole is related to an AMOC decline (Dima & Lohmann, 2010; Rahmstorf et al., 2015), while others conclude that the warming hole cannot be fully attributed to relatively modest AMOC changes in the 20th century (S. Drijfhout et al., 2012; Woollings et al., 2012).

Rahmstorf et al. (2015) (R15 hereafter) argue that the difference between SPG SST and Northern Hemisphere mean surface air temperature (NHT) (a measure of the “warming hole”) reflects AMOC strength changes. To test this hypothesis, R15 perform a linear regression of this surface-temperature based index (STI) against the maximum AMOC strength using MPI-ESM-MR climate model output over the 1850–2100 period. The resulting regression coefficient (2.3 Sv/K) is then used to reconstruct AMOC from instrumental and proxy surface temperature records. However, while the correlation coefficient found by R15 was high (0.90), it was largely determined by out-of-phase trends in NHT and AMOC strength over the strongly greenhouse gas (GHG)-forced 21st century period (their Fig. 2). The AMOC/STI relationship in the model over the 20th century appears significantly weaker.

76 Using 15 CMIP5 models, Caesar et al. (2018) (C18 hereafter) find that the AMOC/STI
77 relationship varies widely across climate models over the 20th century: the ratio of lin-
78 ear trends in AMOC strength to those in a STI (defined as the difference between winter-
79 season SPG SSTs and global mean SST) ranges from -105 to 10 Sv/K across models (0.6
80 to 10 Sv/K for the 12 models determined to have a realistic representation of AMOC;
81 see their extended Table 1). Six CMIP5 models were found to simulate large changes in
82 AMOC (decreases of more than 1.5 Sv) and STI (decreases of more than 0.4 K) over the
83 1870-2016 period, with the other six showing much smaller changes in both quantities.

84 Here, we examine centennial-timescale relationships between sea surface temper-
85 atures, surface air temperatures, and AMOC strength using output from the Commu-
86 nity Earth System Model Large (LE) (Kay et al., 2015) and Single Forcing (SF) (Deser
87 et al., n.d.) Ensembles. These simulations allow AMOC/STI relationships to be assessed
88 under different external forcings, clarifying the origins of discrepancies in scaling coef-
89 ficients and the limitations of STIs as predictors of AMOC changes.

90 **2 Methods**

91 The Community Earth System Model Large (LE) and Single Forcing (SF) Ensem-
92 bles are coordinated numerical simulations of the Earth system conducted using the CESM1
93 climate model, in which the Community Atmosphere Model, version 5, is coupled to the
94 Parallel Ocean Program version 2 (POP2) model at approximately 1° horizontal reso-
95 lution. Additional model components, and details of the model configuration and param-
96 eterizations are more completely described in Kay et al. (2015), and references within.

97 The LE consists of 40 ensemble members. Ensemble member #1 is forced with time-
98 evolving climate forcings (e.g. greenhouse gases, aerosols, ozone, land use changes) over
99 the 1850-2100 period, following an 1801 year control run forced with constant (1850) prein-
100 dustrial forcing. To generate the 40-member initial condition ensemble, perturbations
101 of order 10^{-14} K are applied to the air temperature state of ensemble member #1 on
102 January 1, 1920. Identical external forcing over the 1920-2100 period is the applied to
103 all ensemble members. However, the climate of each ensemble member evolves differently
104 due to differences in the initial state. Taking the arithmetic mean of each quantity across
105 ensemble members allows the identification of an “externally-forced” response. In this

106 analysis, to keep the same number of simulations available for the “all forcings” and sin-
107 gles forcing experiments, we use only LE members #1-20.

108 In the SF ensemble, the same experimental strategy is applied, except a single forc-
109 ing agent (e.g. greenhouse gases) is held at the preindustrial value, allowing an attribu-
110 tion of the changes in climate due to each agent. Here, we examine the changes in quan-
111 tities of interest associated with GHG (greenhouse gas) and AER (industrial aerosol) forc-
112 ing, using the methods of Deser et al. (2020). More details regarding both CESM en-
113 sembles are available in Kay et al. (2015) and Deser et al. (2020).

114 We use the maximum value of the zonally integrated overturning streamfunction
115 north of the Equator in the Atlantic basin, and below 500 m depth, as a metric of AMOC
116 ($AMOC_{MAX}$). We calculate area-averaged SSTs over the SPG region (SST_{SPG} ; Fig. 1,
117 following C18) and the area-averaged northern hemisphere air temperature (NHT; 0° –
118 90° N); the surface temperature index (STI) is defined as the difference between SST_{SPG}
119 and NHT (following R15). Prior to calculating trends and regression coefficients, we re-
120 move drift in CESM-LE by computing a least-squares trend fit to each variable (SST_{SPG} ,
121 NHT and $AMOC_{MAX}$) from the control run. This trend (-1.1×10^{-1} Sv/century for $AMOC_{MAX}$;
122 -1.5×10^{-2} K/century for SST_{SPG} ; -1.4×10^{-3} K/century for NHT) is then removed from
123 individual ensemble members for each variable. Regression coefficients in Table 1 and
124 Supplementary Table 1 are calculated using a geometric mean regression.

125 We compare LE simulations to NHT reconstructions from two datasets: Goddard
126 Institute for Space Studies Surface Temperature Analysis (GISTEMP) and Climate Re-
127 search Unit and Hadley Center Surface Temperature (HadCRUT4). The two datasets
128 are not fully independent; differences stem largely from their treatment of spatial and
129 temporal gaps in the temperature record. SST_{SPG} reconstructions are computed as the
130 spatial mean of SST over the SPG region from two datasets: Extended Reconstructed
131 Sea Surface Temperature (ERSSTv5, generated from International Comprehensive Ocean-
132 Atmosphere Data Set, incorporated to GISTEMP) and Hadley Center Sea Ice and Sea
133 Surface Temperature (HadISST, incorporated into HadCRUT4). Details of these datasets
134 are available elsewhere (Morice et al., 2012; Lenssen et al., 2019).

3 Comparison of CESM-LE output with instrumental-era reconstructions

We first compare temperature anomalies (relative to a 1920-1970 baseline period) from 20 LE members to observational surface temperature reconstructions. The annual mean R15 STI is shown in Fig. 1a; its individual components (SST_{SPG} and NHT, see Methods) are shown in Figs. 1b and 1c, respectively. In the presence of internal variability, individual LE members are not expected to reproduce observations; we thus compare consistency between the range of trends across the simulations and the range of observational estimates. Model output is shown using the ensemble median (to limit the importance of outliers) and uncertainty (the standard deviation across each 20 simulation ensemble).

Observations (orange lines) and LE simulations (blue shading, with the blue line representing ensemble member #1; the only member available over the 1850-1919 period) indicate multidecadal to centennial variability superimposed on substantial higher-frequency variability in all quantities over the 20th century. After 1920, when the LE is initiated, observed variability almost always falls within the range of LE simulations.

Both surface temperature reconstructions and the LE indicate that STI declined over the 20th century. Before ~ 2000 , multidecadal variability is evident in all quantities, in observations and the LE. Subtracting NHT from SST_{SPG} removes some of the shared multidecadal variability in each quantity, leaving the trend most prominent. In the LE, AMOC strength ($AMOC_{MAX}$; see Methods) exhibits multidecadal variability on the order of a few Sv; longer-term trends, while negative, are not significant (-0.94 ± 1.5 Sv/century over the 1921-2000 period; Fig. 1d). In the 21st century in LE (note different axes after 2000), both SST_{SPG} and NHT exhibit large increasing trends (1.1 ± 0.25 and 5.4 ± 0.11 K/century, respectively), opposite in sign to $AMOC_{MAX}$, which decreases by 12.3 ± 0.98 Sv/century.

Over the 1920-2018 period, linear trends in all temperature indices show good agreement between observations and the LE. The LE STI trend is -0.87 ± 0.14 K/century, consistent with observational reconstructions (-0.87 to -1.2 K/century). For SST_{SPG} , the LE trend is -0.11 ± 0.14 K/century, again consistent with observational estimates (-0.11 and 0.02 K/century). In both the reconstructions and the LE, the mean SST_{SPG} trend is small compared to those in STI, and less than its standard deviation across the 20-

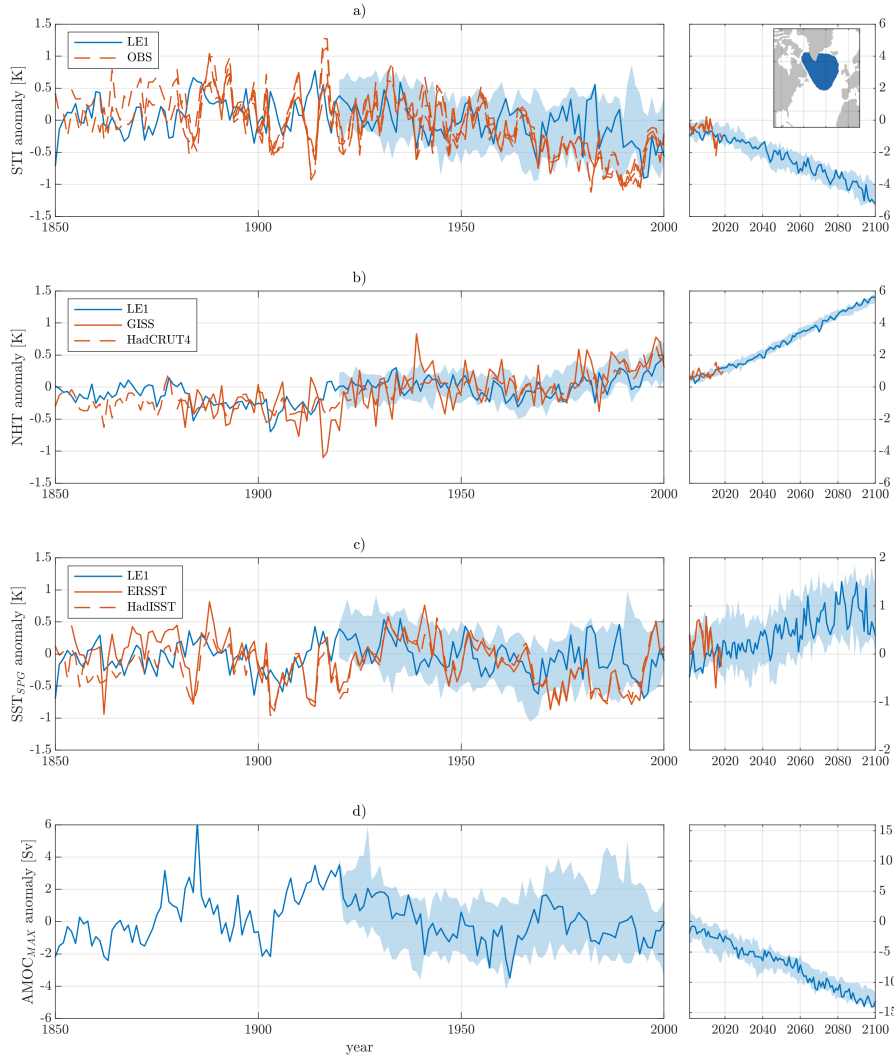


Figure 1. Annual mean a) STI, b) NHT, and c) SST_{SPG} from LE simulations (blue shading is the ensemble range and blue line is ensemble member #1), and various observational reconstructions (orange lines, described in Methods). Since there are two observational products used for NHT and SST_{SPG} , there are 4 STI estimates. Inset in (a) shows the region over which SST_{SPG} is calculated (blue shading). d) Annual mean $AMOC_{MAX}$ (in Sv) from LE simulation #1. All values are anomalies from a 1920-1970 baseline. Note axes scales are different before and after 2000.

167 member ensemble, whereas NHT trends are almost always positive and similar in mag-
 168 nitude to STI trends. This comparison thus indicates that: 1) CESM-LE trends in sur-
 169 face temperature indices are consistent with the range of observed trends over the 1920-
 170 2018 period, and 2) STI is predominantly controlled by increases in NHT, rather than
 171 SST changes in the warming hole region. The latter result weakens the argument that
 172 the STI is dynamically related to AMOC changes.

173 **4 Forcing-dependence of AMOC/STI relationships**

174 We examine the AMOC/STI relationship for each LE member using a linear regression-
 175 based approach over the 1921-2080, 1921-2000, and 2001-2080 periods (see Table 1 and
 176 Methods). For direct comparison with R15, we perform the same analysis for ensemble
 177 member #1 over the 1850-2100 period. Linear regression over the 1921-2080 period shows
 178 a strong AMOC/STI relationship ($r_{STI}^2=0.91\pm 0.01$) with a coefficient (α_{STI}) of 3.0 ± 0.01
 179 Sv/K (slightly higher than the value found by R15 using the MPI-MR model, with a sim-
 180 ilar correlation coefficient). However, regression coefficients differ substantially between
 181 1921-2000 (ensemble mean 4.0 Sv/K) and 2001-2080 (ensemble mean 2.8 Sv/K). There
 182 is a sharp contrast in the significance of the regression coefficient between the 1921-2000
 183 and 2001-2080 periods, with the earlier period indicating a very weak relationship ($r^2=0.05\pm 0.09$).

184 The AMOC/STI relationship over the entire period is thus largely controlled by
 185 the trends over the 21st century. Furthermore, when the relationship is strong (i.e. the
 186 21st century), the AMOC/STI relationship is controlled by the NHT; in fact, the inclu-
 187 sion of SST_{SPG} degrades the fit relative to NHT alone ($r_{STI}^2=0.89\pm 0.02$; $r_{NHT}^2=0.94\pm 0.02$).

188 Externally-forced regression coefficients differ between the 20th and 21st centuries
 189 ($\alpha_{STI}=3.6$ and $\alpha_{STI}=2.8$, respectively). To more clearly identify the origin of this dif-
 190 ference, we utilize the SF ensemble, in which we can separately examine AMOC/STI re-
 191 lationships associated with each of the dominant 20th century forcings: greenhouse gases
 192 (GHG) and industrial aerosols (AER). Time series of STI, NHT, SST_{SPG} , and $AMOC_{MAX}$
 193 are shown for 20 LE, GHG, and AER simulations in Fig. 2 (shading indicates the $\pm 1\sigma$
 194 range across each ensemble, lines indicate the ensemble mean, which approximates the
 195 externally-forced response). Although unforced decadal to multidecadal variability is present
 196 in all simulations, particularly in SST_{SPG} and $AMOC_{MAX}$, externally-forced variations
 197 are most evident at the longest (centennial) timescales. Externally-forced trends in SST_{SPG}

Table 1. Trends in $AMOC_{MAX}$ and STI for each LE simulation, and coefficients (α) and goodness-of-fit (r^2) for regressions of $AMOC_{MAX}$ against STI and NHT. Each column shows the median $\pm 1\sigma$ range across the LE simulations. Externally-forced (ensemble mean) values for the LE and SF simulations are shown in the lower panel.

table1.pdf

198 are generally negligible relative to internal variability, with the exception of a GHG-forced
 199 increase in the second half of the 21st century. Trends in STI are, as in the “all-forcings”
 200 simulations, consistently dominated by trends in NHT.

201 As expected, greenhouse gas forcing leads to increases in NHT and declines in $AMOC_{MAX}$
 202 through the entire simulation (S. S. Drijfhout & Hazeleger, 2007; S. Drijfhout et al., 2008).
 203 The temporal evolution of surface temperature and AMOC strength is more complex un-
 204 der aerosol forcing: in the 20th century, increasing aerosol concentrations drive decreases
 205 in NHT and increases in $AMOC_{MAX}$ (Delworth & Dixon, 2006; Menary et al., 2013),
 206 especially over the 1950-2000 period. In the 21st century, reductions in aerosol concen-
 207 trations after ~ 2000 are associated with trends in the AMOC and STI of similar mag-
 208 nitude but of opposite sign. Thus, AER- and GHG- induced changes are counteracting
 209 in the 20th century and reinforcing in the 21st century; the magnitude of AER-induced
 210 AMOC changes is comparable to GHG-induced changes in both periods.

211 Regression of the GHG-forced STI on $AMOC_{MAX}$ (Table 1) reveals that coefficients
 212 are different in the 20th ($\alpha_{STI}=2.8$ Sv/K) and 21st ($\alpha_{STI}=1.9$ Sv/K) centuries; signif-
 213 icance levels are slightly higher for the 21st century compared to the 20th century ($r_{STI}^2=0.86$
 214 and $r_{STI}^2=0.74$, respectively). Regression coefficients for AER forcing are of compara-
 215 ble magnitude ($\alpha_{STI}=3.7-3.8$ Sv/K) and significance ($r_{STI}^2=0.82-0.86$) in the 20th and
 216 21st centuries. The regression coefficients are larger for AER than for GHG, reflecting
 217 a larger AMOC change per unit NHT change under AER forcing.

218 Differences between externally-forced 20th and 21st century AMOC/STI relation-
 219 ships thus originate from: 1) unique relationships between AMOC and surface temper-
 220 ature under AER and GHG forcing; 2) nonstationary relationships under GHG forcing;
 221 and 3) the time-varying relative importance of each forcing. When AER and GHG forc-
 222 ing drive offsetting NHT and AMOC trends (the 20th century), surface temperature and
 223 AMOC changes are very small. This leads to an overall regression coefficient that is very
 224 sensitive to unforced SST and/or AMOC variability (see next section). The 21st cen-
 225 tury relationship is less sensitive to internal variability, given larger externally-forced trends
 226 and the reinforcing nature of AER and GHG forcing. However, the AMOC/STI rela-
 227 tionship should be expected to vary in time, due both to the evolution of each forcing
 228 agent and the non-stationary AMOC/STI relationship under GHG forcing.

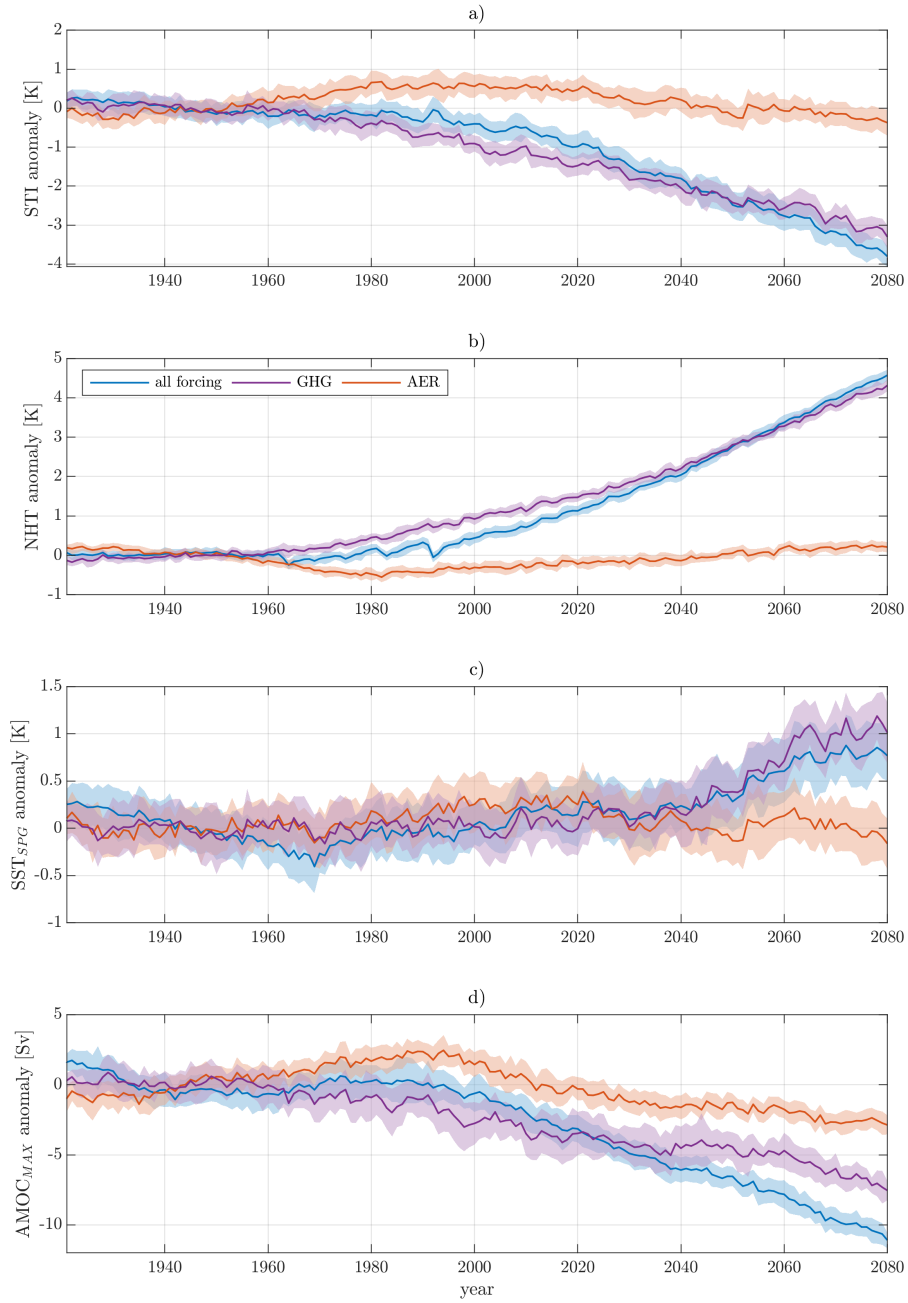


Figure 2. a) STI, b) SST_{SFG}, c) NHT and d) AMOC_{MAX} over the 1920-2080 period for different LE and SF experiments. Ensemble mean is shown with thick lines; shading represents median $\pm 1\sigma$ range.

5 Is the “warming hole” an indicator of AMOC changes?

The previous sections show that centennial-timescale changes in STIs are controlled by large-scale (hemispheric or global), externally-forced, temperature trends. Although this result indicates that previously proposed STIs do not capture a dynamical relationship between the AMOC and SPG SSTs, it does not conflict with the prevalent idea that a “warming hole” is related to AMOC weakening (see introduction).

In the LE, a warming hole is present in both 20th and 21st century simulations, associated with an externally forced decline in $AMOC_{MAX}$ (Figs. 3a and 3d). More generally, the presence of a SST change in the SPG opposite in sign to the radiative forcing is a consistent feature of externally-forced climate changes: for example, increases in AER forcing and $AMOC_{MAX}$ during the 20th century are associated with warming in the SPG interior. Yet despite the consistent appearance of a warming hole under external forcing, SPG SSTs are a poor indicator of the magnitude of AMOC strength changes: SST changes due to the radiative effects of external forcing and AMOC strength counteract each other, and the degree to which they offset is forcing-dependent.

The externally-forced spatial pattern of SST trends also varies with forcing and time period. For example, the 20th century GHG-forced SST pattern (Fig. 3b) bears resemblance to that under 20th century AER forcing, but the GHG-forced “warming hole” shifts eastward in the 21st century (Fig. 3e), suggestive of an shift of the North Atlantic Current (Zhang et al., 2019). 21st century GHG forcing also results in cooling in the Northern Recirculation Gyre/Gulf Stream Extension region (Saba et al., 2016; Caesar et al., 2018), opposite in sign to the enhanced local warming evident in GHG-forced simulations in the 20th century.

When externally-forced trends are small (as in the 20th century, when AER and GHG forcings offset), the SST/ $AMOC_{MAX}$ relationship is highly sensitive to differences resulting from internal variability. SST and $AMOC_{MAX}$ trends vary widely across individual members of the LE over the 1921-2000 period (Fig. 4 and Supplementary Table 2), and are often opposite in sign to the externally-forced change: individual simulations show positive AMOC trends (e.g. LE #3), insignificant and/or positive SST_{SPG} trends (e.g. LE #15), and a negative trend ratio (e.g. LE #4; AMOC trends out-of-phase with SST_{SPG}). There is no obvious relationship between SSTs and $AMOC_{MAX}$ trends

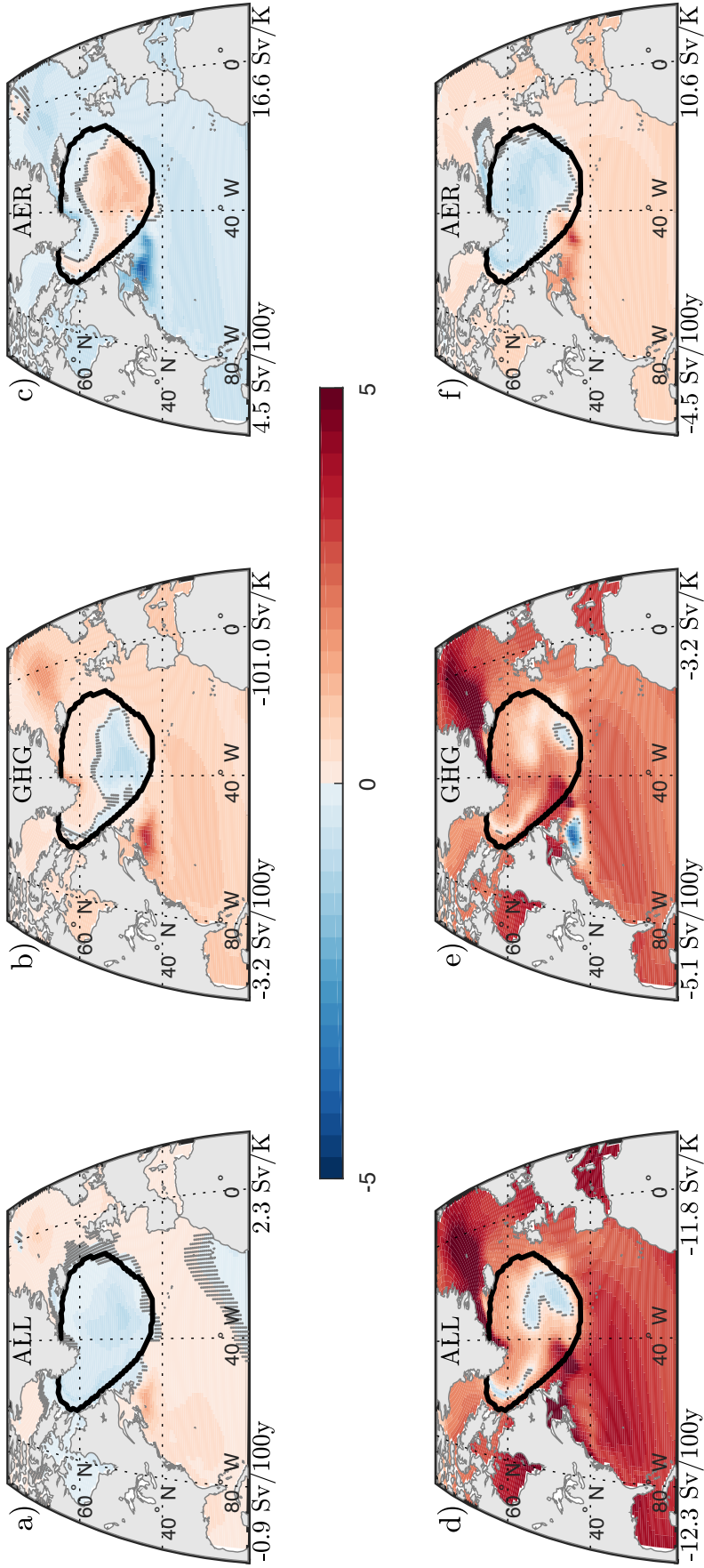


Figure 3. a-c) Ensemble mean local SST trends (K/100y) over the 1921-2000 period: a) LE; b) GHG; c) AER. d-f) as (a-c), for the 2001-2080 period. Values shown below each panel indicate (left) the ensemble mean linear trend in $AMOC_{MAX}$ and (right) the ratio of the ensemble mean linear trend in $AMOC_{MAX}$ to the ensemble mean linear trend in SST_{SPG} . Stippling indicates that the local SST trend is not significant at a 95% confidence level using a Mann-Kendall test.

260 across the ensemble. Over the SPG as a whole, the ensemble standard deviation in the
261 $AMOC_{MAX}/SST_{SPG}$ trend ratio (6.1 Sv/K) is much larger than the LE mean (2.3 Sv/K).

262 Figs. 3 and 4 indicate that the observed trend in North Atlantic SSTs is likely to
263 represent a convolution of AER and GHG-forced responses, and that internal variabil-
264 ity may play a strong role in observed pattern of SST trends and their relationship with
265 AMOC, even over centennial timescales. They also suggest that the inter-model spread
266 in AMOC/STI relationships (as noted in the introduction) is likely to originate in the
267 relative importance of aerosol and GHG-forced responses, as well as differences in ini-
268 tial states.

269 **6 Discussion and Conclusions**

270 Here, using Community Earth System Model ensembles, we have shown that the
271 spatial pattern and magnitude of surface temperature trends associated with changes
272 in AMOC strength, and thus the relationship between AMOC strength and surface-temperature
273 indices, are dependent upon the nature of external forcing. In the 20th century, externally-
274 forced trends in AMOC and SPG SSTs are of a comparable magnitude as those asso-
275 ciated with natural climate system variability. Our results suggest that previously pro-
276 posed STIs are not dynamically related to AMOC strength over centennial timescales;
277 rather, their correlation predominantly reflects opposing trends in AMOC and hemispheric
278 or global surface temperature in response to common external forcing. In formulations
279 proposed to date, STIs are thus poor predictors of AMOC trends outside of their cal-
280 ibration period, calling into question previous interpretations of 20th century AMOC vari-
281 ability (Rahmstorf et al., 2015; Caesar et al., 2018).

282 It is possible that SSTs in a more geographically limited region may be more closely
283 related to oceanic processes, including AMOC. Indeed, the southern SPG consistently
284 shows the largest (out-of-phase with AMOC strength) SST change in Fig. 3. However,
285 the absolute change in SSTs is insufficient as an AMOC metric: for example, there is a
286 small warming in these regions under 21st century GHG forcing (Fig. 3e), even under
287 a dramatic AMOC decline.

288 Our conclusions do not preclude the utility of surface-temperature-based indices to
289 capture AMOC variability on multidecadal timescales (Medhaug & Furevik, 2011; Roberts
290 et al., 2013; Muir & Fedorov, 2015; Kim et al., 2018); such an assessment deserves fur-

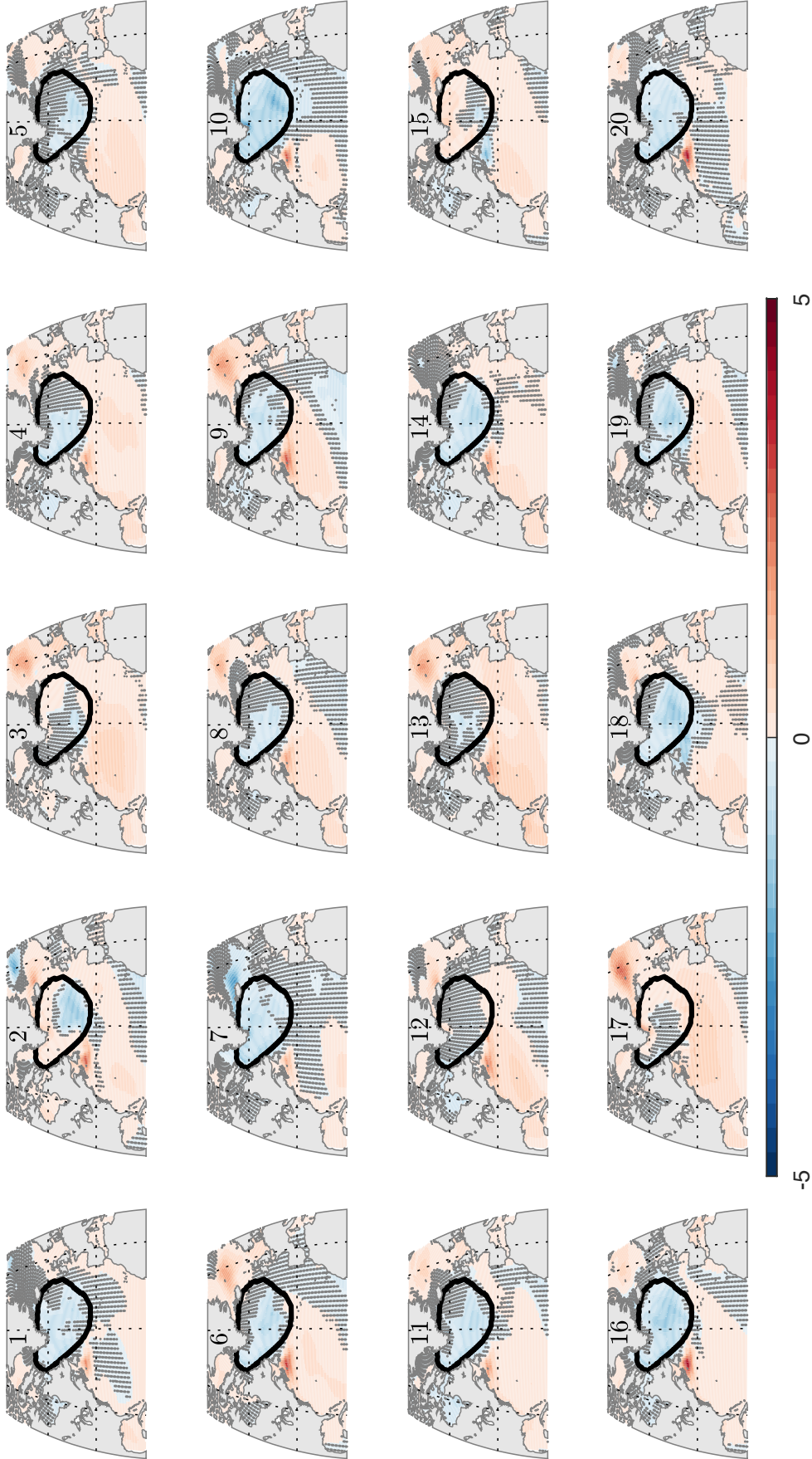


Figure 4. As Fig. 3, but for each of the 20 LE members. For each ensemble member, linear trends in $AMOC_{MAX}$, and the ratio of the linear trend in $AMOC_{MAX}$ to the linear trend in SST_{SPG} , are shown in Supplementary Table 2.

291 ther investigation. With respect to efforts to reconstruct climate and AMOC over longer
292 timescales, other proxies may serve as indicators of AMOC, such as subsurface densi-
293 ties (Roberts et al., 2013), silt records (Thornalley et al., 2018), Florida Current strength
294 (Lund et al., 2006; Gu et al., 2020) or instrumental and proxy-derived coastal sea level
295 records (Kopp, 2013; Kemp et al., 2017; Piecuch, 2020).

296 Our results reveal aspects of AMOC and SST (co-)variability deserving of further,
297 more mechanistically-oriented, model analyses, including forcing- and time-dependent
298 North Atlantic AMOC/SST relationships, and a high sensitivity of AMOC to 20th and
299 21st century aerosol forcing. The sensitivity of AMOC to aerosol forcing is likely to be
300 related to aerosolcloud interactions, which are parameterized and potentially overesti-
301 mated in current-generation climate models (e.g. Menary et al., 2020, and references within).
302 More broadly, our results are conditional on the adequate representation of relevant physics
303 in a coarse-resolution climate model, including: 1) cloud physics, beyond their role in aerosol
304 indirect effects; and 2) ocean mesoscale processes, which are likely to influence AMOC
305 and SST patterns. For some applications (including changes in Gulf Stream position and
306 AMOC strength), models with increased horizontal resolution have been shown to ex-
307 hibit qualitatively different responses to forcing (e.g. Saba et al., 2016; Hirschi et al., 2020).
308 These caveats imply that the relationship and robustness of the forced response should
309 be investigated with other, ideally high-resolution, climate models. However, such com-
310 putationally expensive models may not have the capability to fully investigate the role
311 of natural variability highlighted in this study.

312 **Acknowledgments**

313 CML and MZ acknowledge funding support from NSF Grant OCE1805029. MWB ac-
314 knowledges funding support from the NOAA ESS program (NA16OAR4310167) and the
315 NASA physical oceanography program (NNX17AH49G). The authors thank LuAnne Thomp-
316 son and an anonymous reviewer for their insightful suggestions, and appreciate the ex-
317 tensive effort of National Center for Atmospheric Research (NCAR), the CESM Project,
318 and CISL supercomputing resources (doi:10.5065/D6RX99HX) to produce and make avail-
319 able CESM-LE and SF output. All CESM output used in this paper is available via NCAR.

320 **References**

321 Bjerknes, J. (1964). Atlantic air-sea interaction. In *Advances in geophysics* (Vol. 10,

- 322 pp. 1–82). Elsevier.
- 323 Buckley, M. W., & Marshall, J. (2016, mar). *Observations, inferences, and mecha-*
 324 *nisms of the Atlantic Meridional Overturning Circulation: A review* (Vol. 54)
 325 (No. 1). Blackwell Publishing Ltd. doi: 10.1002/2015RG000493
- 326 Buckley, M. W., Ponte, R. M., Forget, G., & Heimbach, P. (2014, July). Low-
 327 Frequency SST and Upper-Ocean Heat Content Variability in the North At-
 328 lantic. *Journal of Climate*, *27*(13), 4996–5018. Retrieved 2018-06-26, from
 329 <http://journals.ametsoc.org/doi/abs/10.1175/JCLI-D-13-00316.1> doi:
 330 10.1175/JCLI-D-13-00316.1
- 331 Buckley, M. W., Ponte, R. M., Forget, G., & Heimbach, P. (2015, May). Determin-
 332 ing the Origins of Advective Heat Transport Convergence Variability in the
 333 North Atlantic. *Journal of Climate*, *28*(10), 3943–3956. Retrieved 2018-06-26,
 334 from <http://journals.ametsoc.org/doi/10.1175/JCLI-D-14-00579.1> doi:
 335 10.1175/JCLI-D-14-00579.1
- 336 Caesar, L., Rahmstorf, S., Robinson, A., Feulner, G., & Saba, V. (2018). Observed
 337 fingerprint of a weakening Atlantic Ocean overturning circulation. *Nature*,
 338 *556*(7700), 191–196. doi: 10.1038/s41586-018-0006-5
- 339 Chen, D., Busalacchi, A. J., & Rothstein, L. M. (1994). The roles of vertical mix-
 340 ing, solar radiation, and wind stress in a model simulation of the sea surface
 341 temperature seasonal cycle in the tropical Pacific Ocean. *Journal of Geophys-*
 342 *ical Research: Oceans*, *99*(C10), 20345–20359. doi: [https://doi.org/10.1029/](https://doi.org/10.1029/94JC01621)
 343 94JC01621
- 344 Clement, A., Bellomo, K., Murphy, L. N., Cane, M. A., Mauritsen, T., Rdel, G.,
 345 & Stevens, B. (2015). The Atlantic Multidecadal Oscillation without a role
 346 for ocean circulation. *Science*, *350*(6258), 320–324. (Publisher: American
 347 Association for the Advancement of Science)
- 348 De Boer, A. M., Gnanadesikan, A., Edwards, N. R., & Watson, A. J. (2010). Merid-
 349 ional density gradients do not control the atlantic overturning circulation.
 350 *Journal of Physical Oceanography*, *40*(2), 368–380.
- 351 Delworth, T. L., & Dixon, K. W. (2006). Have anthropogenic aerosols delayed
 352 a greenhouse gas-induced weakening of the North Atlantic thermohaline
 353 circulation? *Geophysical Research Letters*, *33*(2), L02606. Retrieved
 354 2020-05-05, from <http://doi.wiley.com/10.1029/2005GL024980> doi:

- 355 10.1029/2005GL024980
- 356 Delworth, T. L., Zhang, R., & Mann, M. E. (2007). Decadal to centennial vari-
 357 ability of the atlantic from observations and models. *Geophysical Monograph-*
 358 *American Geophysical Union, 173*, 131.
- 359 Deser, C., Alexander, M. A., Xie, S.-P., & Phillips, A. S. (2010). Sea surface temper-
 360 ature variability: Patterns and mechanisms. *Annual review of marine science*,
 361 *2*, 115–143.
- 362 Deser, C., Phillips, A. S., Simpson, I. R., Rosenbloom, N., Coleman, D., Lehner,
 363 F., ... Stevenson, S. (n.d.). Isolating the Evolving Contributions of An-
 364 thropogenic Aerosols and Greenhouse Gases: A New CESM1 Large En-
 365 semble Community Resource. *J. Climate, in review*. Retrieved from
 366 [http://www.cgd.ucar.edu/staff/cdeser/docs/submitted.deser.single_](http://www.cgd.ucar.edu/staff/cdeser/docs/submitted.deser.single_forcing_ensemble.feb20.pdf)
 367 [forcing_ensemble.feb20.pdf](http://www.cgd.ucar.edu/staff/cdeser/docs/submitted.deser.single_forcing_ensemble.feb20.pdf)
- 368 Dima, M., & Lohmann, G. (2010, January). Evidence for Two Distinct Modes
 369 of Large-Scale Ocean Circulation Changes over the Last Century. *Journal of*
 370 *Climate, 23*(1), 5–16. Retrieved 2020-06-22, from [https://doi.org/10.1175/](https://doi.org/10.1175/2009JCLI2867.1)
 371 [2009JCLI2867.1](https://doi.org/10.1175/2009JCLI2867.1) doi: 10.1175/2009JCLI2867.1
- 372 Drijfhout, S., Hazeleger, W., Selten, F., & Haarsma, R. (2008, March). Fu-
 373 ture changes in internal variability of the Atlantic Meridional Overturning
 374 Circulation. *Climate Dynamics, 30*(4), 407–419. Retrieved 2020-05-05,
 375 from <http://link.springer.com/10.1007/s00382-007-0297-y> doi:
 376 [10.1007/s00382-007-0297-y](http://link.springer.com/10.1007/s00382-007-0297-y)
- 377 Drijfhout, S., van Oldenborgh, G. J., & Cimadoribus, A. (2012, December). Is
 378 a Decline of AMOC Causing the Warming Hole above the North Atlantic
 379 in Observed and Modeled Warming Patterns? *Journal of Climate, 25*(24),
 380 8373–8379. Retrieved 2020-05-18, from [http://journals.ametsoc.org/doi/](http://journals.ametsoc.org/doi/10.1175/JCLI-D-12-00490.1)
 381 [10.1175/JCLI-D-12-00490.1](http://journals.ametsoc.org/doi/10.1175/JCLI-D-12-00490.1) doi: 10.1175/JCLI-D-12-00490.1
- 382 Drijfhout, S. S., & Hazeleger, W. (2007, April). Detecting Atlantic MOC Changes
 383 in an Ensemble of Climate Change Simulations. *Journal of Climate, 20*(8),
 384 1571–1582. Retrieved 2020-05-05, from [http://journals.ametsoc.org/doi/](http://journals.ametsoc.org/doi/10.1175/JCLI4104.1)
 385 [10.1175/JCLI4104.1](http://journals.ametsoc.org/doi/10.1175/JCLI4104.1) doi: 10.1175/JCLI4104.1
- 386 Frankignoul, C. (1985). Sea surface temperature anomalies, planetary waves, and
 387 airsea feedback in the middle latitudes. *Reviews of geophysics, 23*(4), 231–246.

- 388 doi: <https://doi.org/10.1029/RG023i004p00357>
- 389 Gu, S., Liu, Z., & Wu, L. (2020, March). Time Scale Dependence of the Merid-
390 ional Coherence of the Atlantic Meridional Overturning Circulation. *Journal of*
391 *Geophysical Research: Oceans*, *125*(3). Retrieved 2020-04-14, from [https://](https://onlinelibrary.wiley.com/doi/abs/10.1029/2019JC015838)
392 onlinelibrary.wiley.com/doi/abs/10.1029/2019JC015838 doi: 10.1029/
393 2019JC015838
- 394 Gulev, S. K., Latif, M., Keenlyside, N., Park, W., & Koltermann, K. P. (2013).
395 North atlantic ocean control on surface heat flux on multidecadal timescales.
396 *Nature*, *499*(7459), 464.
- 397 Hirschi, J. J., Barnier, B., Bning, C., Biastoch, A., Blaker, A. T., Coward, A., ...
398 Xu, X. (2020, April). The Atlantic Meridional Overturning Circulation in
399 HighResolution Models. *Journal of Geophysical Research: Oceans*, *125*(4).
400 Retrieved 2020-09-11, from [https://onlinelibrary.wiley.com/doi/abs/](https://onlinelibrary.wiley.com/doi/abs/10.1029/2019JC015522)
401 [10.1029/2019JC015522](https://onlinelibrary.wiley.com/doi/abs/10.1029/2019JC015522) doi: 10.1029/2019JC015522
- 402 Kay, J. E., Deser, C., Phillips, A., Mai, A., Hannay, C., Strand, G., ... Vertenstein,
403 M. (2015, August). The Community Earth System Model (CESM) Large
404 Ensemble Project: A Community Resource for Studying Climate Change
405 in the Presence of Internal Climate Variability. *Bulletin of the Ameri-*
406 *can Meteorological Society*, *96*(8), 1333–1349. Retrieved 2019-03-08, from
407 <http://journals.ametsoc.org/doi/10.1175/BAMS-D-13-00255.1> doi:
408 10.1175/BAMS-D-13-00255.1
- 409 Kemp, A. C., Kegel, J. J., Culver, S. J., Barber, D. C., Mallinson, D. J., Leorri, E.,
410 ... others (2017). Extended late holocene relative sea-level histories for north
411 carolina, usa. *Quaternary Science Reviews*, *160*, 13–30.
- 412 Kim, W. M., Yeager, S., Chang, P., & Danabasoglu, G. (2018). Low-frequency North
413 Atlantic climate variability in the community earth system model large ensem-
414 ble. *Journal of Climate*, *31*(2), 787–813. doi: 10.1175/JCLI-D-17-0193.1
- 415 Kopp, R. E. (2013). Does the mid-atlantic united states sea level acceleration hot
416 spot reflect ocean dynamic variability? *Geophysical Research Letters*, *40*(15),
417 3981–3985.
- 418 Kravtsov, S., & Spannagle, C. (2008). Multidecadal climate variability in observed
419 and modeled surface temperatures. *Journal of Climate*, *21*(5), 1104–1121.
- 420 Lenssen, N. J., Schmidt, G. A., Hansen, J. E., Menne, M. J., Persin, A., Ruedy, R.,

- 421 & Zys, D. (2019). Improvements in the GISTEMP uncertainty model. *Journal of Geophysical Research: Atmospheres*, *124*(12), 6307–6326. (Publisher:
422 Wiley Online Library)
- 423
- 424 Lund, D. C., Lynch-Stieglitz, J., & Curry, W. B. (2006, November). Gulf Stream
425 density structure and transport during the past millennium. *Nature*,
426 *444*(7119), 601–604. Retrieved 2018-06-27, from [http://www.nature.com/
427 articles/nature05277](http://www.nature.com/articles/nature05277) doi: 10.1038/nature05277
- 428 Marshall, J., Scott, J. R., Armour, K. C., Campin, J.-M., Kelley, M., & Romanou,
429 A. (2015, April). The oceans role in the transient response of climate to abrupt
430 greenhouse gas forcing. *Climate Dynamics*, *44*(7-8), 2287–2299. Retrieved
431 2020-05-18, from <http://link.springer.com/10.1007/s00382-014-2308-0>
432 doi: 10.1007/s00382-014-2308-0
- 433 Medhaug, I., & Furevik, T. (2011). North Atlantic 20th century multidecadal
434 variability in coupled climate models: Sea surface temperature and ocean over-
435 turning circulation. *Ocean Science*, *7*(3), 389–404. doi: 10.5194/os-7-389-2011
- 436 Menary, M. B., Roberts, C. D., Palmer, M. D., Halloran, P. R., Jackson, L., Wood,
437 R. A., ... Lee, S.-K. (2013, April). Mechanisms of aerosol-forced AMOC
438 variability in a state of the art climate model: HISTORICALLY STRENGTH-
439 ENING AMOC. *Journal of Geophysical Research: Oceans*, *118*(4), 2087–2096.
440 Retrieved 2018-06-27, from <http://doi.wiley.com/10.1002/jgrc.20178>
441 doi: 10.1002/jgrc.20178
- 442 Menary, M. B., Robson, J., Allan, R. P., Booth, B. B. B., Cassou, C., Gastineau, G.,
443 ... Zhang, R. (2020, July). AerosolForced AMOC Changes in CMIP6 Histor-
444 ical Simulations. *Geophysical Research Letters*, *47*(14). Retrieved 2020-09-11,
445 from <https://onlinelibrary.wiley.com/doi/abs/10.1029/2020GL088166>
446 doi: 10.1029/2020GL088166
- 447 Morice, C. P., Kennedy, J. J., Rayner, N. A., & Jones, P. D. (2012, April). Quanti-
448 fying uncertainties in global and regional temperature change using an ensem-
449 ble of observational estimates: The HadCRUT4 data set: THE HADCRUT4
450 DATASET. *Journal of Geophysical Research: Atmospheres*, *117*(D8), n/a–n/a.
451 Retrieved 2018-06-27, from <http://doi.wiley.com/10.1029/2011JD017187>
452 doi: 10.1029/2011JD017187
- 453 Muir, L. C., & Fedorov, A. V. (2015, dec). How the AMOC affects ocean tem-

- 454 peratures on decadal to centennial timescales: the North Atlantic versus
 455 an interhemispheric seesaw. *Climate Dynamics*, 45(1-2), 151–160. doi:
 456 10.1007/s00382-014-2443-7
- 457 Pardo, X. A. P. M. G. L. F.-B., Paula C., & Prez, F. F. (2011). Evolution of
 458 upwelling systems coupled to the long-term variability in sea surface tem-
 459 perature and Ekman transport. *Climate Research*, 48(2-3), 231–246. doi:
 460 <https://doi.org/10.3354/cr00989>
- 461 Piecuch, C. (2020). Weakening of the gulf stream at florida straits over the past
 462 century inferred from coastal sea-level data. *Earth and Space Science Open*
 463 *Archive*, 84. Retrieved from <https://doi.org/10.1002/essoar.10502506.1>
 464 doi: 10.1002/essoar.10502506.1
- 465 Rahmstorf, S., Box, J. E., Feulner, G., Mann, M. E., Robinson, A., Rutherford, S.,
 466 & Schaffernicht, E. J. (2015). Exceptional twentieth-century slowdown in
 467 atlantic ocean overturning circulation. *Nature climate change*, 5(5), 475–480.
- 468 Roberts, C. D., Garry, F. K., & Jackson, L. C. (2013). A multimodel study of sea
 469 surface temperature and subsurface density fingerprints of the Atlantic merid-
 470 ional overturning circulation. *Journal of Climate*, 26(22), 9155–9174. doi:
 471 10.1175/JCLI-D-12-00762.1
- 472 Saba, V. S., Griffies, S. M., Anderson, W. G., Winton, M., Alexander, M. A., Del-
 473 worth, T. L., ... others (2016). Enhanced warming of the north west a
 474 tlantic ocean under climate change. *Journal of Geophysical Research: Oceans*,
 475 121(1), 118–132.
- 476 Thornalley, D. J., Oppo, D. W., Ortega, P., Robson, J. I., Brierley, C. M., Davis, R.,
 477 ... Keigwin, L. D. (2018). Anomalously weak Labrador Sea convection and
 478 Atlantic overturning during the past 150 years. *Nature*, 556(7700), 227–230.
 479 doi: 10.1038/s41586-018-0007-4
- 480 Webster, P. J., Holland, G. J., Curry, J. A., & Chang, H.-R. (2005). Changes in
 481 tropical cyclone number, duration, and intensity in a warming environment.
 482 *Science*, 309(5742), 1844–1846. doi: 10.1126/science.1116448
- 483 Williams, R. G., Roussenov, V., Smith, D., & Lozier, M. S. (2014). Decadal evolu-
 484 tion of ocean thermal anomalies in the north atlantic: The effects of ekman,
 485 overturning, and horizontal transport. *Journal of Climate*, 27(2), 698–719.
- 486 Winton, M., Griffies, S. M., Samuels, B. L., Sarmiento, J. L., & Frierich, T. L.

- 487 (2013, April). Connecting Changing Ocean Circulation with Changing Cli-
488 mate. *Journal of Climate*, 26(7), 2268–2278. Retrieved 2020-05-18, from
489 <http://journals.ametsoc.org/doi/10.1175/JCLI-D-12-00296.1> doi:
490 10.1175/JCLI-D-12-00296.1
- 491 Woollings, T., Harvey, B., Zahn, M., & Shaffrey, L. (2012, December). On the role
492 of the ocean in projected atmospheric stability changes in the Atlantic polar
493 low region. *Geophysical Research Letters*, 39(24), 2012GL054016. Retrieved
494 2020-05-18, from [https://onlinelibrary.wiley.com/doi/abs/10.1029/](https://onlinelibrary.wiley.com/doi/abs/10.1029/2012GL054016)
495 [2012GL054016](https://onlinelibrary.wiley.com/doi/abs/10.1029/2012GL054016) doi: 10.1029/2012GL054016
- 496 Zhang, R., Sutton, R., Danabasoglu, G., Kwon, Y.-O., Marsh, R., Yeager, S., ...
497 Little, C. (2019). A review of the role of the atlantic meridional overturning
498 circulation in atlantic multidecadal variability and associated climate impacts.
499 *Reviews of Geophysics*, 57(2), 316–375.

Table 1

| forcing | period | Δ AMOC [Sv/century] | Δ STI [K/century] | STI [Sv/K] | r^2_{STI} | NHT [Sv/K] | r^2_{NHT} |
|------------------------------------|-----------|-------------------------------|-----------------------------|---------------|-----------------|----------------|-----------------|
| all-forcing (large) ensemble | 1921-2080 | -7.0 \pm 0.4 | -2.3 \pm 0.1 | 3.0 \pm 0.1 | 0.91 \pm 0.01 | -2.5 \pm 0.1 | 0.93 \pm 0.01 |
| | 1921-2000 | -0.7 \pm 1.5 | -0.7 \pm 0.2 | 4.0 \pm 1.7 | 0.05 \pm 0.09 | 6.6 \pm 5.9 | 0.02 \pm 0.04 |
| | 2001-2080 | -12.6 \pm 1.2 | -4.2 \pm 0.3 | 2.8 \pm 0.2 | 0.89 \pm 0.02 | -2.3 \pm 0.2 | 0.94 \pm 0.02 |
| LE #1 | 1850-2100 | -0.5 | -0.2 | 3.1 | 0.91 | -2.6 | 0.92 |

Externally-Forced (ensemble mean)

| forcing | period | Δ AMOC [Sv/century] | Δ STI [K/century] | STI [Sv/K] | r^2_{STI} | NHT [Sv/K] | r^2_{NHT} |
|-------------|-----------|-------------------------------|-----------------------------|---------------|-------------|---------------|-------------|
| all-forcing | 1921-2000 | -0.9 | -0.7 | 3.6 | 0.29 | -5.0 | 0.01 |
| | 2001-2080 | -12.3 | -4.3 | 2.8 | 0.98 | -2.3 | 0.98 |
| GHG | 1921-2000 | -3.2 | -1.2 | 2.8 | 0.74 | -2.8 | 0.78 |
| | 2001-2080 | -5.1 | -2.7 | 1.9 | 0.86 | -1.2 | 0.88 |
| AER | 1921-2000 | 4.5 | 1.2 | 3.7 | 0.86 | -4.6 | 0.85 |
| | 2001-2080 | -4.5 | -1.2 | 3.8 | 0.82 | -6.1 | 0.80 |

Figure 1.

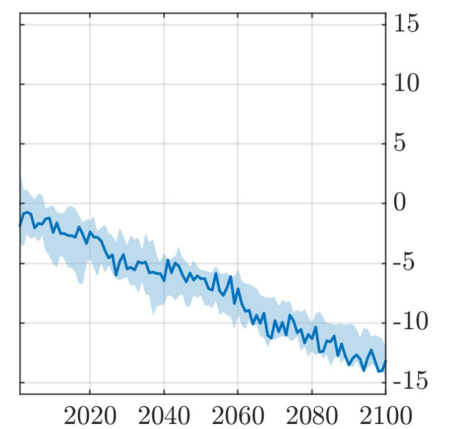
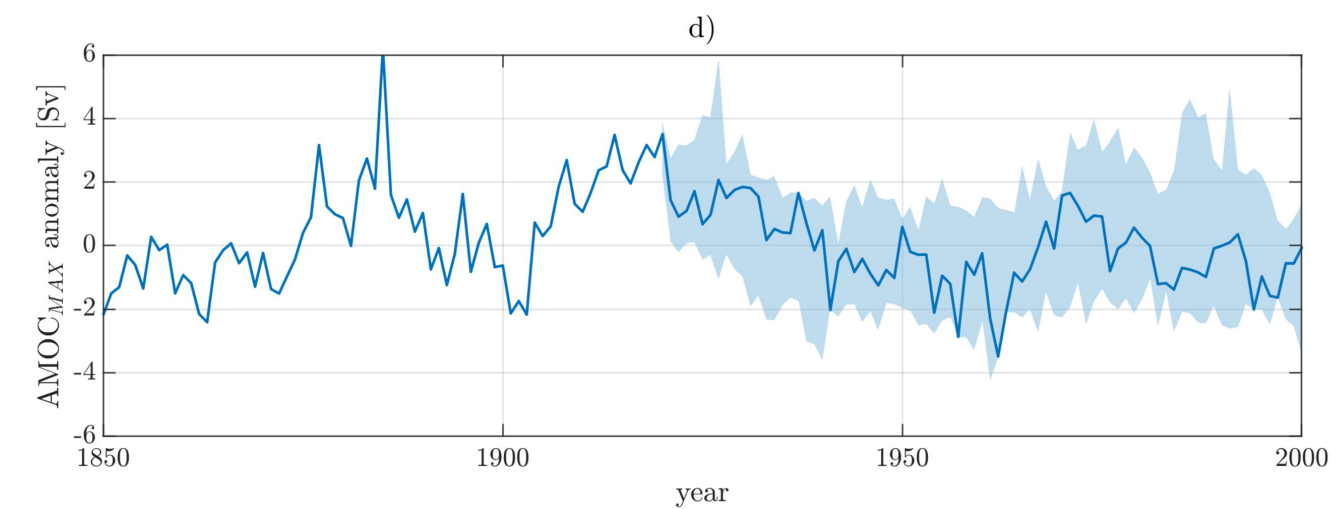
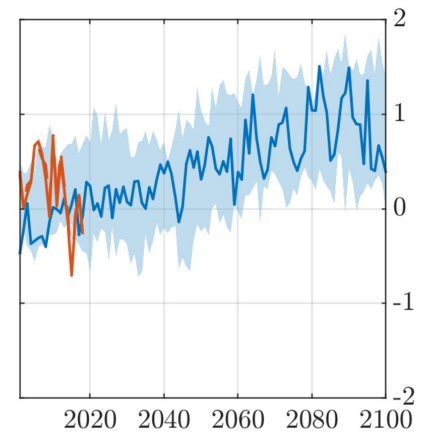
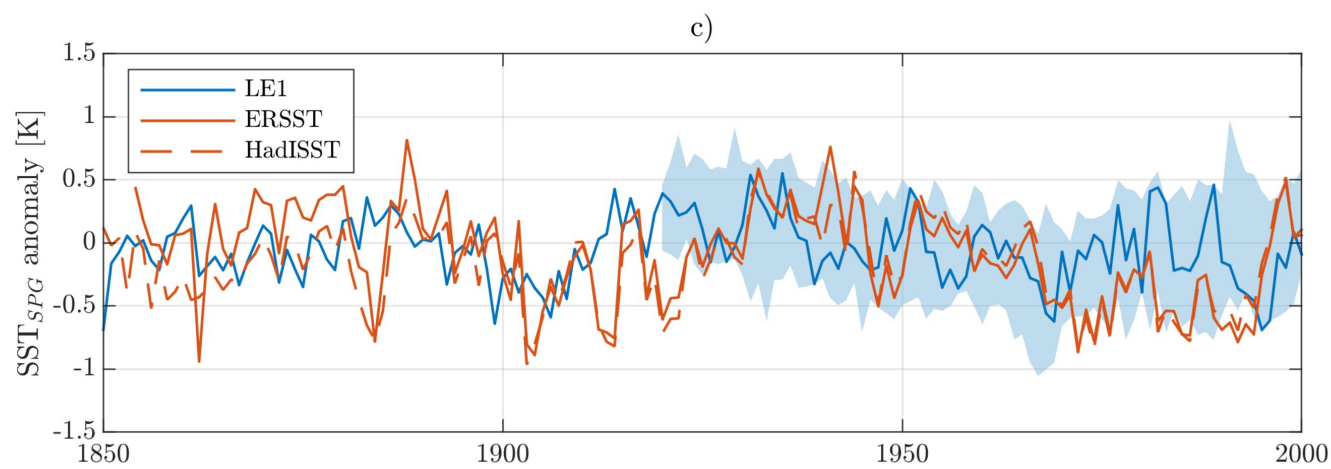
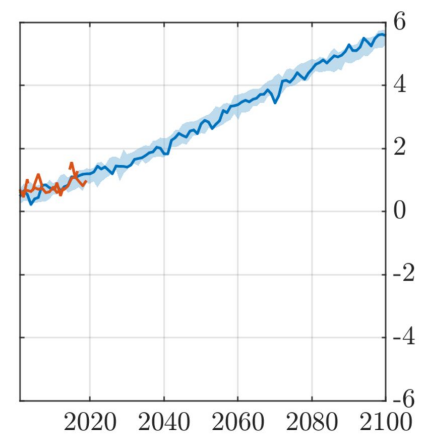
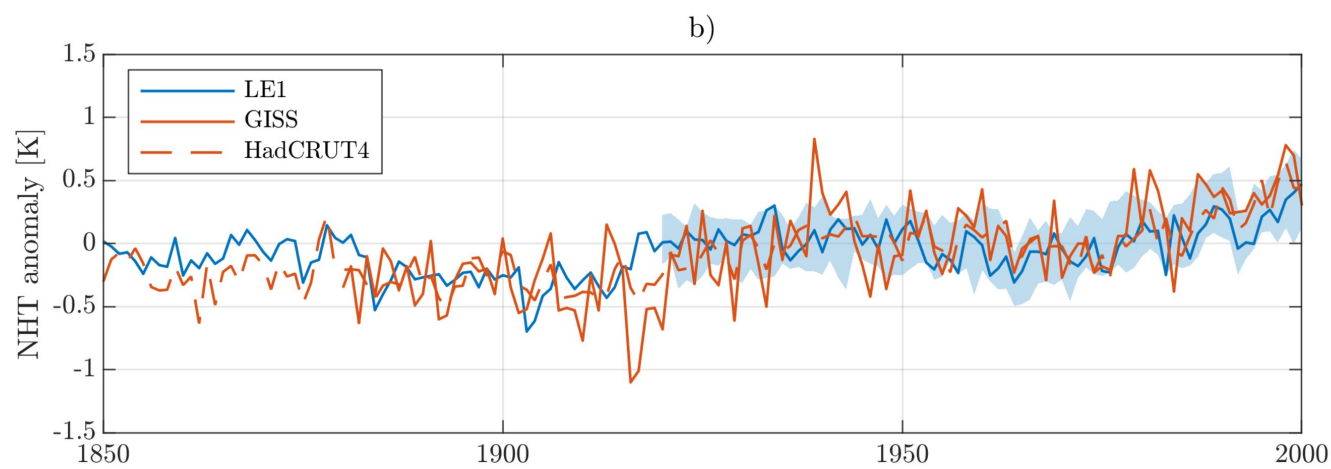
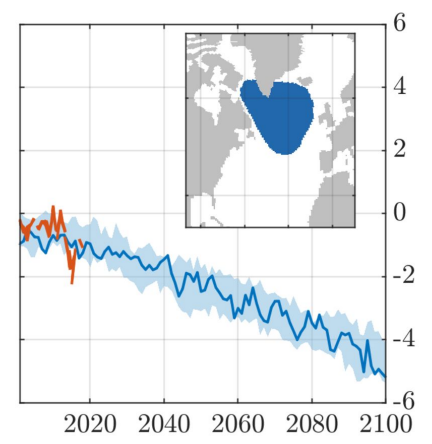
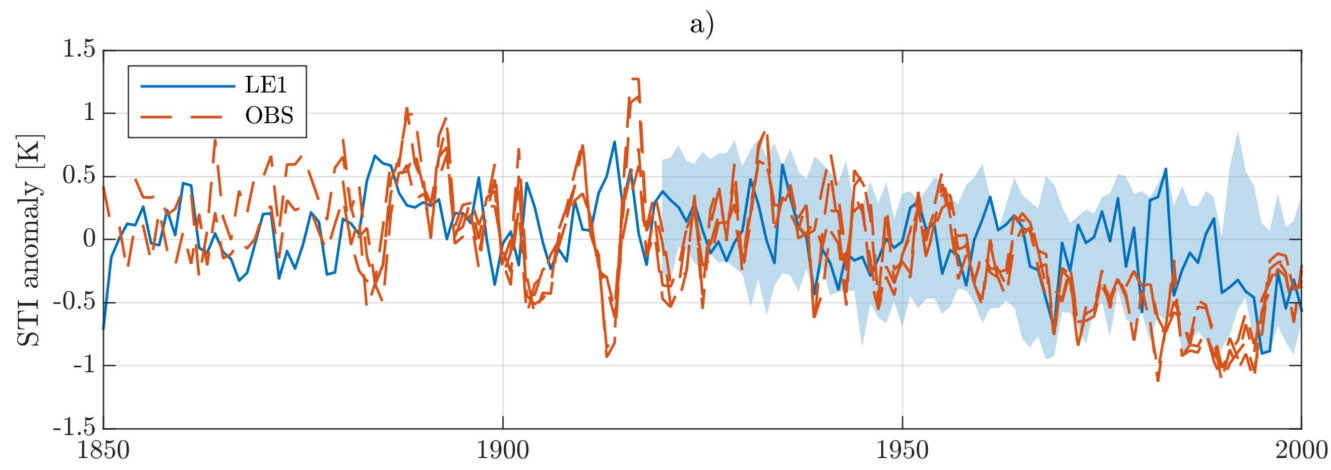


Figure 2.

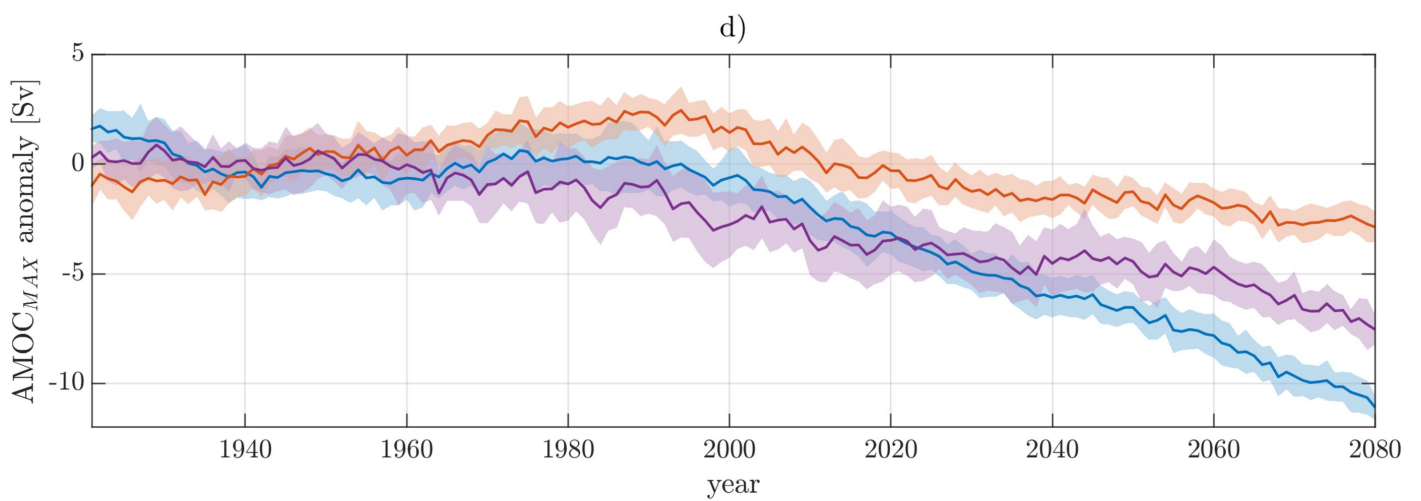
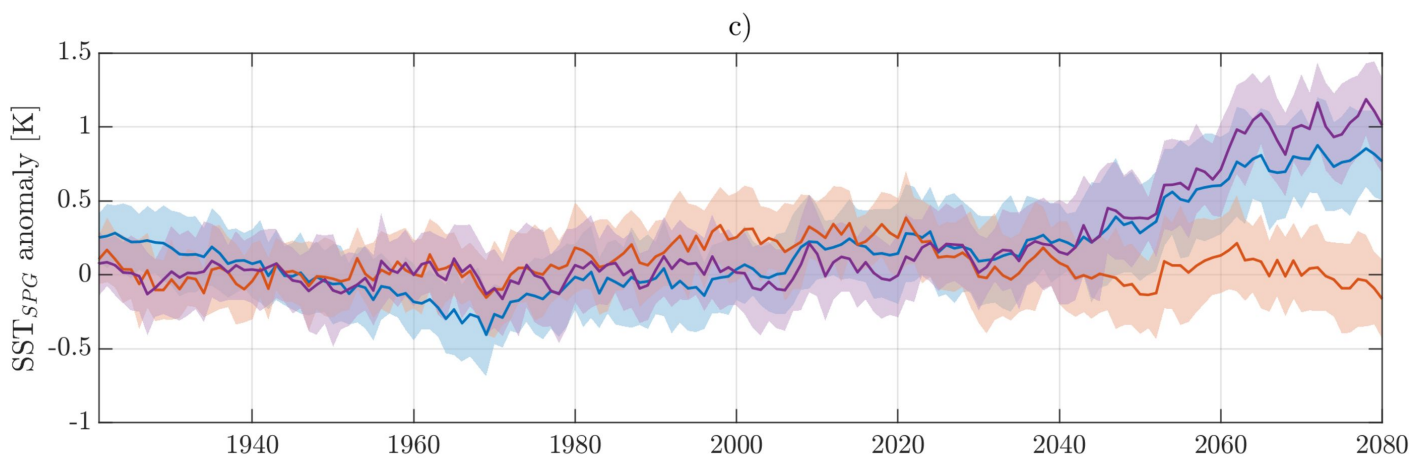
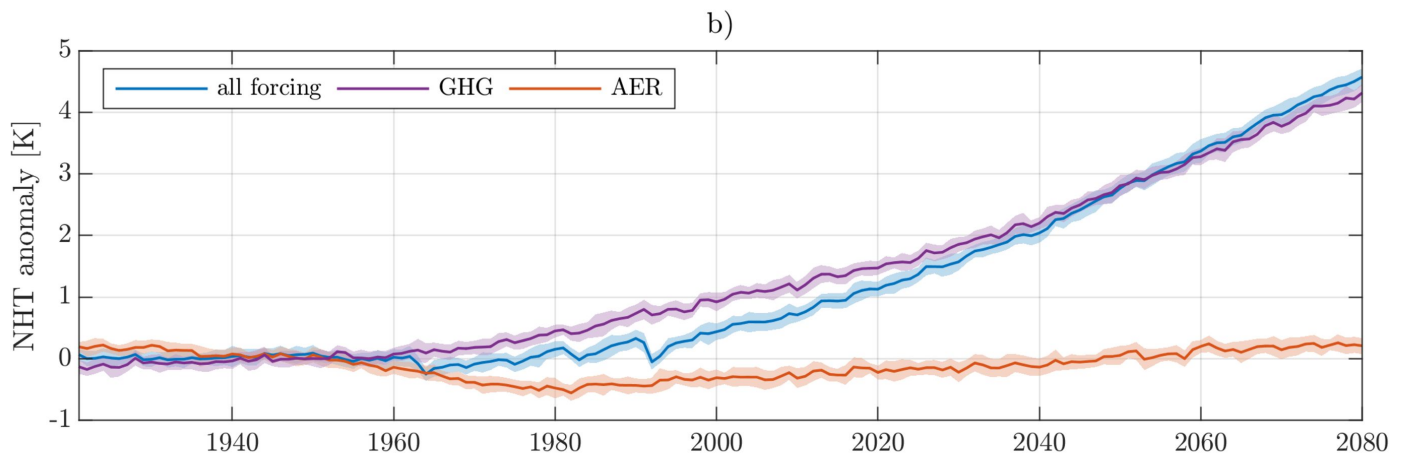
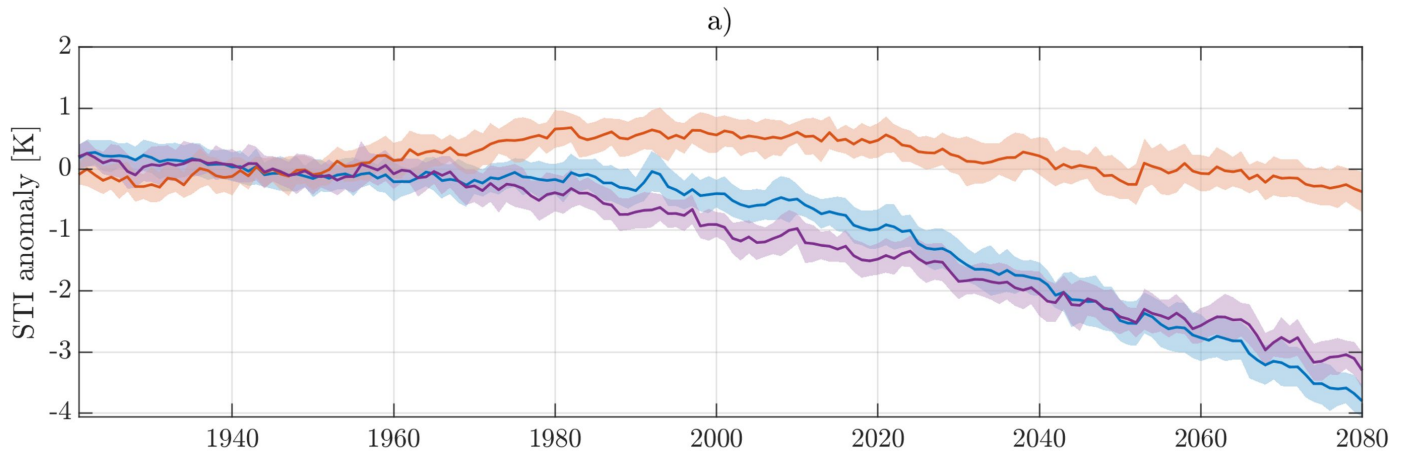


Figure 3.

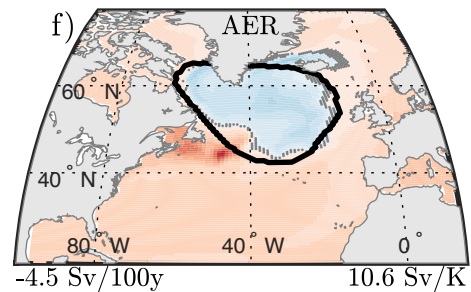
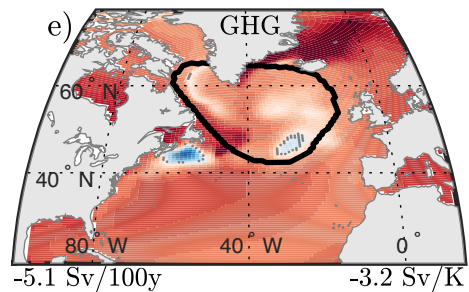
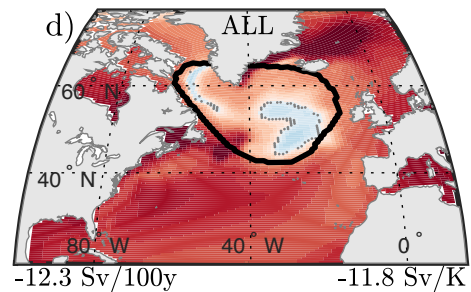
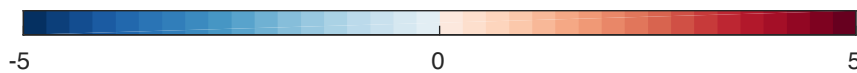
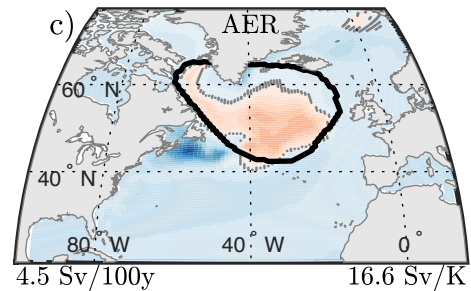
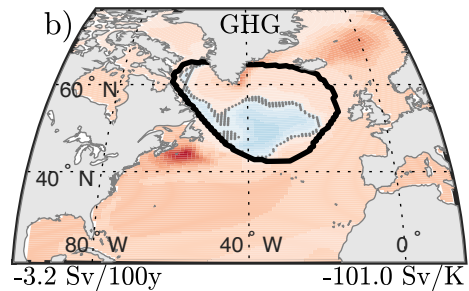
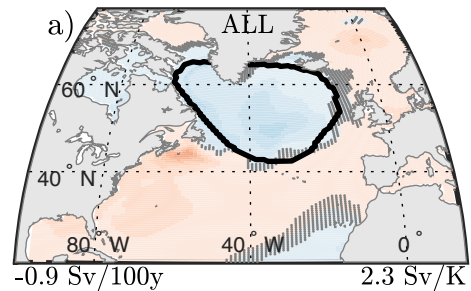


Figure 4.

